

Environmental Science Water Research & Technology

Accepted Manuscript

This article can be cited before page numbers have been issued, to do this please use: A. Pedregal-Montes, E. Jennings, R. Marcé and M. J. Farré, *Environ. Sci.: Water Res. Technol.*, 2026, DOI: 10.1039/D6EW00128A.



This is an Accepted Manuscript, which has been through the Royal Society of Chemistry peer review process and has been accepted for publication.

Accepted Manuscripts are published online shortly after acceptance, before technical editing, formatting and proof reading. Using this free service, authors can make their results available to the community, in citable form, before we publish the edited article. We will replace this Accepted Manuscript with the edited and formatted Advance Article as soon as it is available.

You can find more information about Accepted Manuscripts in the [Information for Authors](#).

Please note that technical editing may introduce minor changes to the text and/or graphics, which may alter content. The journal's standard [Terms & Conditions](#) and the [Ethical guidelines](#) still apply. In no event shall the Royal Society of Chemistry be held responsible for any errors or omissions in this Accepted Manuscript or any consequences arising from the use of any information it contains.

Water Impact Statement: This study shows that the ability to provide safe drinking water is strongly influenced by upstream climate variability, reservoir dynamics, and operational decisions that shape disinfection by-product formation risk. The findings highlight the need to manage source waters and reservoirs as active control points, supporting more resilient and integrated strategies to safeguard water supplies under increasing hydroclimatic uncertainty.



1 **Integrating catchment, climate and reservoir drivers to estimate the risk of THM**
2 **formation at a drinking water treatment plant inlet**

New Article Online
DOI: 10.1039/D6EW00128A

3
4 **Angela Pedregal-Montes^{a,b*}, Eleanor Jennings^c, Rafael Marcé^d, Maria José Farré^a**

5
6 ^aCatalan Institute for Water Research (ICRA), Carrer Emili Grahit 101, Parc Científic i Tecnològic de
7 la Universitat de Girona, 17003 Girona, Spain

8 ^bUniversity of Girona, Plaça de Sant Domènec 3, 17004 Girona, Spain

9 ^cCentre for Freshwater and Environmental Studies, Dundalk Institute of Technology, A91 K584
10 Dundalk, Ireland

11 ^dCentre for Advanced Studies of Blanes (CEAB), Spanish National Research Council (CSIC), 17300
12 Blanes, Spain

13
14 *Corresponding author.

15 Email address: apedregal@icra.cat (A. Pedregal-Montes)

16
17 **Abstract**

18 Using long-term monitoring and machine learning, this study links upstream
19 hydrometeorology, reservoir processes, and operations to source water conditions relevant to
20 trihalomethane (THM) formation risk at the Mediterranean Ter drinking water treatment plant
21 (DWTP) in Spain, supplied by a three-reservoir cascade (Sau-Susqueda-Pasteral). Based on
22 exploratory analyses, three target variables were selected as indicators of THM formation risk:



23 dissolved organic carbon (DOC) and water temperature (WT) at the DWTP inlet and
24 fluorescent dissolved organic matter (fDOM) at the Susqueda withdrawal depth. Permutation
25 importance results using Random Forest and LSTM models indicated that withdrawal-layer
26 conditions at Susqueda dominate downstream variability: DOC was most strongly associated
27 with extracted fDOM and other withdrawal water quality variables, whereas inlet WT was
28 primarily controlled by Susqueda withdrawal temperature. For fDOM at Susqueda, reservoir
29 storage volume emerged as a major driver, highlighting the influence of water availability,
30 retention time, and stratification on DOM dynamics. Optimized LSTM models predicted the
31 three target variables with strong validation skill (R^2 and KGE > 0.8). Scenario simulations
32 identified seasonal windows of opportunity for THM risk reduction, with selective withdrawal
33 targeting low-fDOM or cooler layers reducing indicator-based THM formation risk at the
34 DWTP inlet, particularly during warm stratified periods and post-summer rainfall transitions.
35 The effectiveness of this strategy was event-dependent and constrained by reservoir levels and
36 gate accessibility. These results highlight opportunities to reduce DBP formation risk through
37 upstream management, supporting a shift from end-of-pipe control to multi-barrier strategies,
38 particularly in regions facing increasing hydroclimatic stress.

39 **Keywords:** source water quality, source water management, disinfection by-products,
40 machine learning, Mediterranean

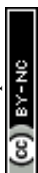
41

42

43

44

45



46 1. Introduction

View Article Online
DOI: 10.1039/D6EW00128A

47 Surface water supplies for drinking water are experiencing increasing pressure from various factors,
48 including climate change, escalating water demand, and diverse human activities, with direct
49 consequences for both water availability and raw water quality ¹⁻³. In chlorinated drinking water
50 treatment plants (DWTP), utilities must balance effective disinfection with the need to limit disinfection
51 by-products (DBPs), which form when disinfectants react with natural organic matter and inorganic
52 constituents (e.g., halides) present in source waters ⁴. Due to their potential long-term health effects ^{5,6},
53 more DBP species are being regulated in drinking water (Directive (EU) 2020/2184). Among DBPs,
54 trihalomethanes (THMs) remain the most widely monitored and well-characterized group, yet because
55 many other (often unregulated) DBPs may pose equal or greater toxicological concern ⁷, treatment
56 plants are increasingly shifting from reactive compliance responses to proactive management of
57 precursor conditions ⁸⁻¹⁰.

58 Operational control therefore often focuses on monitoring source water precursor indicators at the
59 DWTP inlet using dissolved organic matter (DOM) surrogates such as dissolved organic carbon (DOC),
60 ultraviolet absorbance at 254 nm (UV₂₅₄), or fluorescent DOM (fDOM), together with variables that
61 influence formation kinetics, such as water temperature. These indicators are commonly incorporated
62 into site-specific DBP risk tools to support operational decisions ¹¹. However, rapid shifts in source
63 water conditions such as temperature spikes, hydrologic events, or precursor pulses can reduce the
64 response time available to operators and compromise water safety ¹²⁻¹⁴. A key limitation of many DBP
65 predictive tools is that they are primarily DWTP centered and may not explicitly account for upstream
66 drivers of DOM and water temperature, including catchment forcing, reservoir processes, and water
67 source management ¹⁵. This gap is particularly relevant in Mediterranean regions, where droughts and
68 intense rainfall are projected to intensify, with strong implications for DOM dynamics in rivers and
69 reservoirs ¹⁶⁻¹⁸. Understanding the link between upstream controls and inlet indicators is therefore
70 essential for more anticipatory and climate-adaptive management from source to tap.

71 Linking upstream forcing to source water conditions at a DWTP inlet requires methods that can
72 represent both catchment driven inputs and managed reservoir transformations at relevant time scales



73 19. This is challenging because DOM dynamics reflect interacting hydrological, physical and
74 biogeochemical processes ^{20,21}, while catchment DOM monitoring is typically low frequency (often
75 monthly). Process-based hydrological and biogeochemical models can help bridge this gap by providing
76 temporally continuous estimates of catchment DOM and discharge ²², but downstream water quality
77 reaching the DWTP additionally reflects nonlinear interactions among meteorology, reservoir
78 stratification and internal processing, and selective withdrawal operations that are difficult to
79 parameterize explicitly in complex, highly managed reservoir systems ²³. In this context, machine
80 learning (ML) approaches offer a practical alternative for forecasting operationally relevant source
81 water indicators, as they can learn empirical, potentially lagged and nonlinear relationships directly
82 from multi-source monitoring and operational datasets without requiring explicit representation of all
83 underlying processes ²⁴.

84 Previous work at the Ter DWTP showed that DOC and raw water temperature measured at the plant
85 inlet can be used as practical indicators to classify THM formation risk using an empirical risk matrix,
86 as raw waters are predominantly influenced by DOM and typically show low contributions from
87 inorganic precursors (e.g., bromide) ²⁵. This framework reflects pre-treatment THM formation risk,
88 defined as the potential for DBP formation during subsequent disinfection based on source water
89 conditions. Building on this approach, this study examines the upstream controls, predictability, and
90 operational leverage points governing these indicators in the Mediterranean Ter river-reservoir-DWTP
91 continuum supplying the Barcelona metropolitan area. We compiled and analyzed an extensive spatio-
92 temporal dataset spanning catchment forcing, reservoir water quality and stratification, reservoir storage
93 and gate operations, and DWTP inlet monitoring. The dataset was complemented by daily upstream
94 DOC and discharge simulations from a previously validated catchment model to represent inflow
95 variability at appropriate temporal resolution. We first evaluated relationships among DOM proxies and
96 THM observations to support the use of DOC as a consistent indicator, then assessed longitudinal DOC
97 patterns to identify the most influential upstream control points along the continuum. Subsequently, we
98 applied ML-based driver attribution and prediction to quantify the dominant hydrometeorological,
99 water quality, and operational drivers of DOC and water temperature at the DWTP inlet, and finally

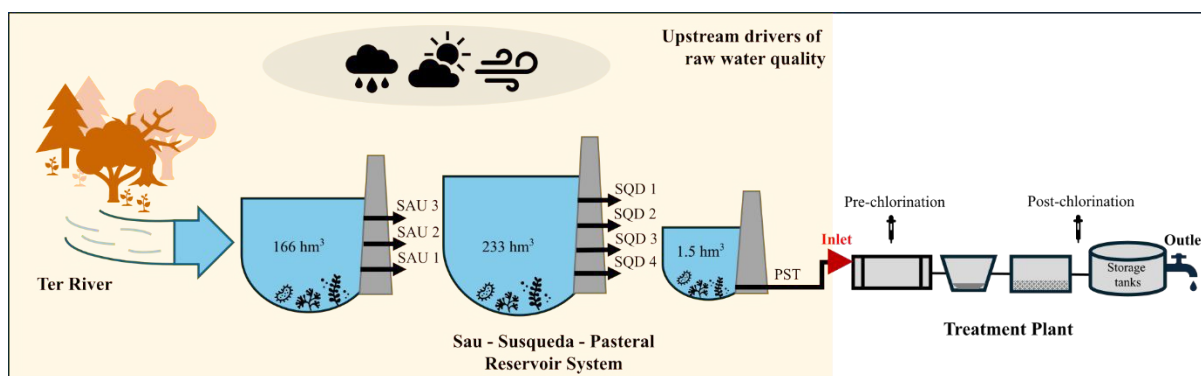


100 tested alternative selective-withdrawal strategies to assess how operational choices could shift
 101 indicator-based THM risk classes. By focusing on source water indicators and their upstream drivers,
 102 the study provides a basis for more anticipatory, climate-adaptive source water management that can
 103 support THM risk mitigation without attempting to directly model DBP formation within the treatment
 104 process.

106 2. Methods

107 2.1. Study area and river-reservoir-DWTP continuum

108 This study focuses on the Ter DWTP, located in Cardedeu, Catalonia (northeastern Spain), operated by
 109 the *Ens d'Abastament d'Aigua Ter-Llobregat* (ATL), which supplies drinking water to the Barcelona
 110 metropolitan area (≈ 4.5 million inhabitants). The DWTP sources raw water from the Ter River Basin,
 111 which drains into a cascade of three reservoirs, Sau, Susqueda and Pasteral, with storage capacities of
 112 166 hm^3 , 233 hm^3 , and 1.5 hm^3 , respectively (Figure 1). A detailed map of the Ter River catchment,
 113 including elevation, river network, and reservoirs, is provided in Figure S1.



114
 115 **Figure 1.** Schematic of the Ter River-reservoir-DWTP continuum showing upstream drivers, reservoir
 116 storage and selective withdrawal at Sau and Susqueda (SQA), bottom withdrawal at Pasteral (PST), and
 117 conventional treatment with pre-chlorination (chlorine dioxide and sodium hypochlorite) and post-
 118 chlorination (sodium hypochlorite) at the DWTP.

119
 120 Reservoir water levels and releases are managed by regional water authorities to accommodate multiple
 121 uses, including hydroelectric generation, ecological flow maintenance, and recreational activities. In
 122 contrast, water quality management is primarily conducted by ATL through selective withdrawal

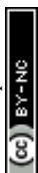


123 operations at the Sau and Susqueda reservoirs, which are equipped with three and four intake levels,
124 respectively (Figure 1; Figures S2-S3). These intake structures allow operators to select withdrawal
125 depth based on water quality conditions; however, the set of available intake levels varies with reservoir
126 water level, which determines the accessibility of individual gates. Water is subsequently withdrawn
127 from the bottom outlet of the Pasteral reservoir, where discharge rates can be regulated, and transported
128 to the DWTP via a pipeline, with an approximate travel time of 12 hours to the DWTP inlet. Additional
129 characteristics of the reservoirs are provided in Table S1. Although the three-reservoir configuration
130 provides substantial buffering of hydrological variability and raw water quality, the system remains
131 sensitive to extreme meteorological conditions that can alter reservoir stratification and organic matter
132 dynamics, thereby influencing raw water quality at the DWTP inlet ²⁶.

133 The Ter DWTP employs a conventional treatment train that includes both pre-chlorination (combined
134 dosing of chlorine dioxide (ClO₂) and sodium hypochlorite (NaClO) to increase oxidation and
135 disinfection capacity) and post-chlorination (NaClO). Pre-chlorination is the stage most susceptible to
136 DBP formation, as disinfectants are applied when organic precursor concentrations in raw water are
137 highest. Consequently, operational control focuses on limiting DBP formation by adjusting disinfectant
138 dosage and treatment conditions in response to raw water characteristics. Previous studies have shown
139 that, at the Ter DWTP, raw water DOM concentration and water temperature are particularly relevant
140 factors influencing THM formation risk, as they control precursor availability and reaction kinetics
141 under local treatment conditions ²⁵. Due to the spatial extent of the supply network and variability in
142 water demand, hydraulic retention times (HRT) within the distribution system range from several hours
143 to multiple days. Therefore, to ensure compliance with drinking water regulations, which establish a
144 maximum allowable concentration of 100 µg L⁻¹ for total THMs at the consumer tap, ATL applies a
145 more conservative internal operational limit of 50 µg L⁻¹ for total THMs at the DWTP outlet.

146 2.2. Study workflow

147 This study followed a structured, multi-step workflow to investigate the upstream controls,
148 predictability, and operational sensitivity of water quality variables associated with THM formation risk
149 at the Ter DWTP inlet.



150 First, exploratory analyses were conducted using long-term monitoring data to characterize the temporal
151 variability of organic matter and water temperature at the DWTP inlet, their relationships with THM
152 concentrations at the outlet, and their connection to upstream hydrometeorological conditions along the
153 river-reservoir-DWTP continuum. These analyses were used to support the selection of candidate water
154 quality indicators and to inform predictor preselection for subsequent modeling. The exploratory
155 analysis leveraged the full monitoring record (2015-2023) to capture long-term variability and
156 hydroclimatic extremes, whereas subsequent ML modeling was constrained to a shorter period defined
157 by the availability of high-frequency reservoir data required to represent key upstream drivers.

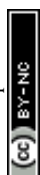
158 Second, ML models were implemented to quantify the relative importance of upstream drivers
159 influencing the selected indicators. Random Forest (RF) and Long Short-Term Memory (LSTM)
160 models were trained using preselected hydrometeorological, operational, and water quality predictors,
161 and permutation importance (PI) was applied to attribute the contribution of individual drivers. Third,
162 LSTM models were refined for each indicator by reducing predictor sets based on driver attribution
163 results and predictive performance. The optimized LSTM models were then used to evaluate
164 predictability and temporal dynamics under observed conditions.

165 Finally, the calibrated LSTM models were applied to simulate alternative reservoir operation scenarios
166 designed to reduce THM formation risk at the DWTP inlet. Model outputs under baseline and scenario
167 conditions were subsequently translated into THM formation risk classes using published empirical
168 relationships.

169 2.3. Data collection and preprocessing

170 Data were collected from multiple locations along the river-reservoir-DWTP continuum to characterize
171 meteorological, hydrological, operational, and water quality variability. Table 1 summarizes the
172 datasets used in the study and their main characteristics.

173 Meteorological forcing was characterized using daily air temperature, total precipitation, and solar
174 radiation obtained from the ERA5 reanalysis product of the European Centre for Medium-Range
175 Weather Forecasts²⁷. ERA5 provides global atmospheric data at a spatial resolution of 0.25°. Data were



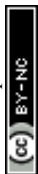
176 extracted for the grid cell encompassing the Ter reservoir system and used to represent atmospheric
 177 drivers influencing catchment processes, reservoir stratification, and water temperature dynamics.

178 Hydrological inputs from the Ter River were represented using daily discharge and DOC concentrations
 179 simulated by the Precipitation, Evapotranspiration, and Runoff Simulator for Solute Transport
 180 (PERSiST; Futter et al., 2014) coupled with the Integrated Catchments Model for Carbon (INCA-C,
 181 INCA-C; Futter et al., 2007), previously validated for the Ter basin³⁰. These simulations were used to
 182 represent upstream catchment inputs and to provide daily values for ML analysis. In addition, observed
 183 DOC concentrations were available at monthly resolution and were used exclusively for exploratory,
 184 continuum-scale analyses.

185 **Table 1.** Overview of datasets used in the study, including location, variables, temporal resolution, data
 186 source, and application in the analysis.

Location	Variable	Temporal resolution	Source	Use in study
Meteorology	Air temperature, total precipitation, solar radiation	Daily	ERA5 reanalysis	Exploratory and ML
	DOC	Monthly	Monitoring records	Exploratory
Ter river	Discharge (simulated)	Daily	Process-based catchment model	Exploratory and ML
	DOC (simulated)	Daily	Process-based catchment model	ML
	fDOM, WT, DO, turbidity, Chl-a	Daily (aggregated from 2-min profiler data)	In situ profilers	ML
Reservoirs	DOC	Monthly	Monitoring records	Exploratory
	Gate operation	Event-based (gate changes)	Reservoir operational records	Exploratory and ML
	Stored volumes	Daily	Reservoir operational records	ML
DWTP inlet	DOC, UV254, SUVA, WT	Daily	DWTP records	Exploratory and ML
DWTP outlet	Total THM concentration	Weekly	DWTP records	Exploratory

187 **Note:** Exploratory analyses used the full monitoring period (1 January 2015-31 December 2023).
 188 Machine learning (ML) models were trained and evaluated over the period constrained by reservoir
 189 profiler availability (4 February 2017-30 November 2020). Abbreviations: DWTP, drinking water
 190 treatment plant; DOC, dissolved organic carbon; fDOM, fluorescent dissolved organic matter; WT,
 191 water temperature; UV254, ultraviolet absorbance at 254 nm; SUVA, specific ultraviolet absorbance;
 192 DO, dissolved oxygen; Chl-a, chlorophyll-a; THM, trihalomethane.



193 Reservoir dynamics were characterized using a combination of monitoring records, high-frequency
194 profiling data, and operational information. Monthly DOC concentrations at the surface and at extracted
195 depths were available for all reservoirs and were used for exploratory analyses. For Sau and Susqueda
196 reservoirs, high-frequency water quality data (2-minute resolution) from profiling buoys installed near
197 the dams were aggregated to daily resolution at the surface (0-5m) and at extraction depths (2.5 m above
198 and below the active gate). At each site, a YSI EXO2 multiprobe recorded turbidity (NTU), chlorophyll-
199 a (Chl-a, mg L⁻¹), dissolved oxygen (DO, mg L⁻¹) water temperature (°C) and fDOM (QSU) throughout
200 the water column. EXO fDOM can be used as a surrogate for colored DOM (CDOM) (excitation 365
201 ± 5 nm; emission 480 ± 40 nm), and raw fDOM data were water temperature corrected following ³¹.
202 Additionally, reservoir operational data, including daily stored volume and gate operation, were used
203 to represent storage dynamics and selective withdrawal. No profiler data were available for the Pastoral
204 reservoir due to its small volume and short HRT (~1 day) relative to Sau and Susqueda. Profiler data
205 availability differed between reservoirs. Susqueda profiler data were available from 4 February 2017 to
206 30 November 2020, whereas Sau profiler data were available from 4 February 2017 to 1 March 2020,
207 after which the instrument failed due to damage sustained during Storm Gloria (19-24 January 2020;
208 Berdalet et al., 2020). Historical time series of selected reservoir variables are available in the
209 Supplementary Material (Figure S2-S3).

210 At the DWTP inlet, historical datasets of raw water quality variables were available daily, including
211 DOC, UV254, specific ultraviolet absorbance (SUVA), and water temperature. At the DWTP outlet,
212 total THM concentrations were measured at weekly resolution and used exclusively for exploratory
213 analyses. Further methodological details for these variables are provided in the Supplementary Material
214 (Text S1).

215 Exploratory analyses were conducted using the full available monitoring period (1 January 2015 – 31
216 December 2023). ML models were trained and evaluated over 4 February 2017 to 30 November 2020,
217 with some gaps, defined by Susqueda profiler availability to retain the Storm Gloria period in the
218 dataset; missing Sau profiler periods within this window were treated as extended gaps in the
219 corresponding predictors. This period was selected to ensure the inclusion of high-frequency reservoir



220 variables required to represent withdrawal-depth water quality and operational dynamics. While it
221 captured substantial hydroclimatic variability, including extreme events, it did not fully encompass the
222 longer-term variability observed in the full monitoring record (2015-2023). Therefore, model results
223 should be interpreted within the range of conditions represented during the model training and
224 evaluation period. All datasets were subjected to quality control and harmonized prior to analysis.
225 Variables used in ML were aligned on a common daily time step; interpolation was applied only to
226 profiler-derived variables to support daily alignment, while all other predictors were already available
227 at daily resolution. Detailed preprocessing procedures are provided in Text S1.

228 **2.4. Exploratory analysis to support variable selection**

229 At the DWTP inlet, DOM was characterized using multiple proxies to represent both organic carbon
230 quantity and quality. DOC was used as a measure of concentration, while UV254 and SUVA were
231 included to capture variations in DOM optical properties. Pearson correlation analysis was applied to
232 assess relationships among DOM proxies, water temperature, and total THM concentrations measured
233 at the DWTP outlet. Hydrometeorological variables, including air temperature, precipitation, river
234 discharge, and reservoir storage volume, were analyzed in parallel with raw water quality variables to
235 provide context for upstream influences on temporal variability at the DWTP inlet.

236 To evaluate spatial patterns in organic matter variability along the continuum, DOC was used as the
237 sole DOM proxy, as it was the only organic matter variable consistently available across all locations.
238 DOC concentrations were compared along the river-reservoir-DWTP continuum using seasonal
239 summaries and correlation analysis; for the Sau and Susqueda reservoirs, DOC values at both surface
240 and extracted depths were considered.

241 **2.5. Machine learning framework**

242 Machine learning models were used to simulate selected water quality variables relevant to THM
243 formation risk assessment and to investigate their upstream drivers. Data-driven approaches are well
244 suited to highly managed aquatic systems, as they can exploit high-frequency monitoring and long-term
245 datasets to learn nonlinear relationships under varying environmental and operational conditions^{24,33}.



246 Two ML approaches were implemented in this study: RF and LSTM neural networks. These models
247 were selected to provide complementary perspectives on driver attribution rather than to perform
248 exhaustive model benchmarking. RF was used as a robust and interpretable baseline method, widely
249 applied in environmental prediction tasks due to its ability to capture nonlinear relationships and handle
250 correlated predictors. In contrast, LSTM networks were selected to represent state-of-the-art sequence
251 modeling approaches, capable of learning temporal dependencies and lagged relationships in time series
252 data.

253 RF is a non-parametric ensemble method that constructs multiple decision trees using bootstrap samples
254 and aggregates their predictions, and has demonstrated strong predictive performance across a range of
255 environmental forecasting applications^{34–37}. LSTM networks were employed to represent temporal
256 dependencies and lagged relationships in time-series data, and have shown strong performance in recent
257 hydrological and water quality forecasting studies^{37–41}.

258 Driver attribution analyses were performed using both RF and LSTM models, while LSTM models
259 were used for forecasting and scenario simulations. Predictor sets were tailored to each modeled
260 variable to reduce redundancy and model complexity. All predictors were aligned to a common daily
261 time step and harmonized prior to modeling (see Text S1). LSTM inputs were constructed using a fixed
262 14-day lookback window. Different window lengths were tested, and a 14-day window yielded the best
263 predictive performance across all target variables. This window length was consistent with the short- to
264 medium-term dynamics of the system. Models were trained and evaluated using a chronological split,
265 with the first 80% of the time series used for training and the remaining 20% reserved as a held-out test
266 period. Model performance was assessed using the coefficient of determination (R^2), root mean squared
267 error (RMSE), mean absolute error (MAE), and Kling-Gupta efficiency (KGE). Reproducibility was
268 ensured by fixing random seeds and enforcing deterministic settings. Additional details on model
269 configuration, hyperparameter selection, and implementation settings are provided in Text S2.

270 2.6. Driver attribution using permutation importance



271 Candidate predictors were preselected for each modeled variable based on exploratory analyses, data
272 availability, and system-specific process understanding, prior to driver attribution. All candidate
273 predictors considered are listed in Table 1; the preselection step retained variables most directly
274 connected to the target locations and dominant processes identified along the continuum.

275 Predictor relevance was quantified using PI, which evaluates the contribution of each predictor
276 by randomly permuting its values and quantifying the resulting change in model performance
277 ³⁴. This approach avoids biases associated with split-based importance measures in the presence
278 of correlated predictors ⁴². Importance was expressed as the percentage change in the
279 coefficient of determination relative to the unpermuted model (ΔR^2 , %).

280 PI was computed on the chronologically held-out validation period for both RF and LSTM models.
281 For RF, each predictor was permuted repeatedly and ΔR^2 values were averaged across repetitions. For
282 LSTM, predictors were permuted repeatedly across samples in the test set while keeping the remaining
283 predictors unchanged; permutations were applied at the sequence level to preserve within-sequence
284 temporal structure of non-permuted inputs. Attribution results from RF and LSTM were compared to
285 assess the robustness of driver rankings across static and sequential learning frameworks.

286 Positive ΔR^2 values indicate a loss of predictive skill when a predictor is permuted and therefore
287 denote an important contributor to model performance, whereas values near zero or negative
288 indicate negligible or unstable contributions that may arise from sampling variability and
289 collinearity ⁴³. Predictors were interpreted based on relative ranking and consistency across
290 repetitions, consistent with recommendations for correlated predictors in predictive models ⁴³.
291 As PI can be sensitive to multicollinearity among predictors, importance values may be
292 distributed across correlated variables. Therefore, results were interpreted primarily in terms
293 of relative ranking rather than absolute importance values.

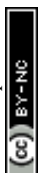
294 2.7. Scenario simulations and THM formation risk estimation



295 Optimized LSTM models were used to simulate alternative reservoir operation scenarios designed to
296 reduce THM formation risk at the DWTP inlet. Scenario simulations were conducted exclusively with
297 LSTM models, given their ability to represent temporal dependencies in predictor time series.

298 Two operational scenarios were defined at the Susqueda reservoir, the last major operational control
299 point upstream of the DWTP, to represent plausible selective-withdrawal strategies designed to
300 influence THM risk indicators (DOC and water temperature) at the DWTP inlet: (i) extraction of water
301 layers characterized by lower organic matter values, and (ii) extraction of the coolest available water
302 layer. These scenarios were implemented by modifying the input time series of reservoir extraction
303 depth and associated profiler-derived water quality variables while keeping all other predictors identical
304 to baseline conditions. Scenario definition was constrained to physically accessible withdrawal layers
305 based on observed profiler data and gate availability under prevailing reservoir water levels. Figure S3
306 illustrates the Susqueda reservoir stratification, water quality, water levels, and gate operation data used
307 to define the scenarios.

308 Scenario predictions were computed only for dates where the required scenario inputs were available
309 for the preceding 14 days (LSTM lookback window); therefore, gaps in scenario trajectories reflect
310 incomplete profiler input data rather than model instability. For each scenario, the optimized LSTM
311 models were used to simulate DOC and water temperature at the DWTP inlet for all eligible dates.
312 Baseline simulations corresponding to observed operational conditions were also produced for
313 comparison. Simulated DOC and water temperature time series were subsequently translated into THM
314 formation risk classes using empirical, expert-based relationships developed previously for the Ter
315 DWTP²⁵. In this framework, DOC and water temperature were first classified into discrete levels based
316 on predefined concentration and temperature ranges (Table S2), and combined THM formation risk
317 classes were then assigned using a rule-based matrix linking these categories (Table S3). These risk
318 classes represent pre-treatment THM formation risk at the DWTP inlet, defined as the potential for DBP
319 formation during subsequent disinfection. Changes in THM formation risk under alternative scenarios
320 were assessed by comparing simulated risk classes against baseline conditions over the simulated
321 period.



322

323 **3. Results and discussion**324 **3.1. Relationships between DWTP inlet conditions and THM concentrations under hydro-**
325 **meteorological variability**

326 The three DOM proxies measured at the DWTP inlet, DOC, UV254 and SUVA, were strongly
327 correlated with each other ($r = 0.63-0.94$; Figures S4-S5), indicating that they conveyed consistent
328 information on DOM dynamics over the study period. Given this strong covariation, and because DOC
329 was the only DOM proxy available consistently along the river-reservoir-DWTP continuum, subsequent
330 analyses focused on DOC as the primary indicator of DOM variability at the DWTP inlet.

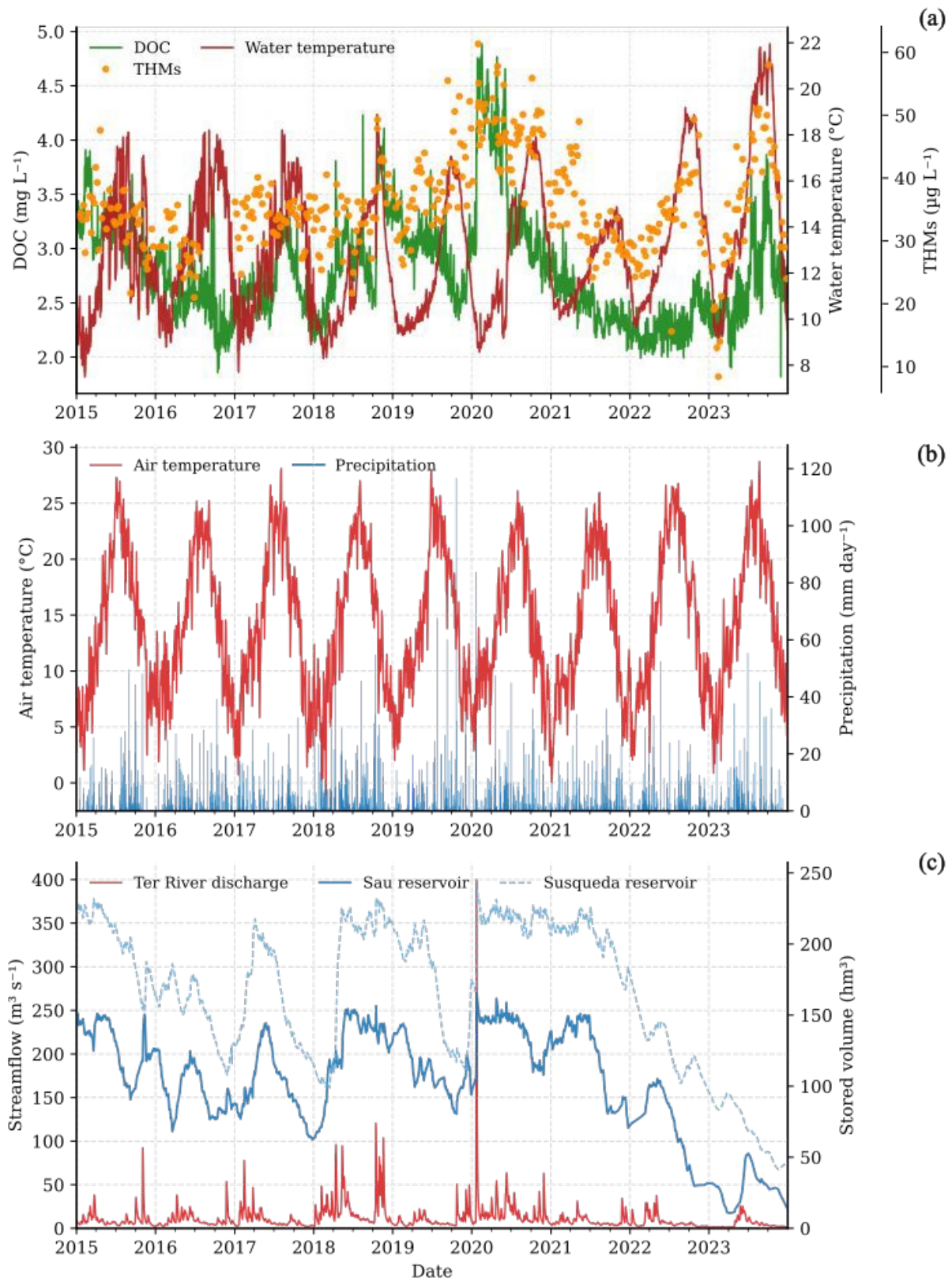
331 The temporal evolution of raw water DOC and water temperature exhibited seasonal variability, while
332 departures from typical cycles were apparent during periods of hydro-meteorological extremes (Figure
333 2a). To place these patterns in context, atmospheric forcing (air temperature and precipitation) and
334 hydrological and operational conditions are shown in Figures 2b-c. Total THM concentrations
335 measured at the DWTP outlet displayed marked temporal variability (Figure 2a) and tended to be higher
336 during periods of elevated DOC and/or higher raw water temperature, although the correspondence was
337 not systematic. Pearson correlation analysis indicated positive but moderate associations between
338 THMs and DOC ($r = 0.39$) and between THMs and water temperature ($r = 0.25$). While these
339 correlations alone do not imply causality, they indicate that DOC and water temperature capture part of
340 the variability associated with THM formation. In this study, these variables were used as operational
341 indicators of pre-treatment THM formation risk at the Ter DWTP inlet, rather than direct predictors of
342 THM concentrations.

343 Several periods highlighted the influence of extreme conditions on inlet water quality and potential
344 THM formation. During Storm Gloria in early 2020, DOC increased abruptly (Figure 2a), concurrent
345 with intense precipitation and hydrological disturbance (Figure 2b-c), likely reflecting enhanced
346 mobilization and transport of catchment-derived organic matter⁴⁴. In contrast, the prolonged drought
347 from 2021 onwards coincided with elevated water temperatures and altered DOC dynamics (Figure 2a),



348 with DOC increases often occurring after rainfall events after extended dry periods, a response
 349 commonly reported in Mediterranean catchments ⁴⁵.

View Article Online
 DOI: 10.1039/D6EW00128A



350



351 **Figure 2.** Time series for the period January 2015-December 2023 showing (a) daily DOC concentrations and water temperature at the DWTP inlet together with weekly total THM
352 concentrations at the DWTP outlet; (b) daily mean air temperature and total precipitation; and (c) daily
353 Ter River discharge and stored volumes of the Sau and Susqueda reservoirs.
354
355

356 Finally, higher THM concentrations observed during the later part of the record (2022-2023; Figure 2a)
357 suggested that THM formation risk during prolonged droughts was influenced not only by upstream
358 hydrological conditions but also by source water management decisions at the system scale. During
359 periods of reduced inflow and elevated temperatures, the Ter DWTP relies on operational adjustments
360 within the reservoir cascade to manage raw water quality, while overall supply reliability is supported
361 through blending of treated surface water with desalinated water prior to storage and distribution. While
362 blending does not alter THM formation during treatment, it may increase bromide in distributed water,
363 promoting the formation of more toxic brominated THMs⁴⁶. Although bromide concentrations and
364 THM speciation were not evaluated in this study, this highlights an important operational consideration
365 for managing DBP precursors in source waters.

366 **3.2. Longitudinal patterns of organic matter along the river-reservoir-DWTP continuum**

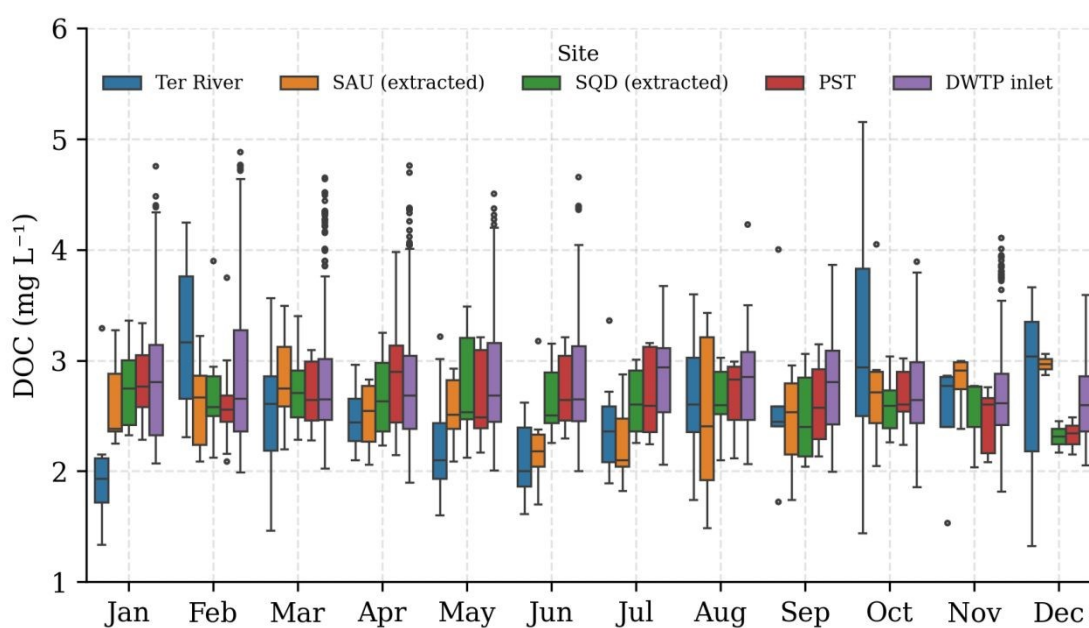
367 DOC distributions revealed systematic spatial and seasonal differences along the continuum (Figure 3).
368 DOC concentrations in the Ter River were generally lower and more variable than in downstream
369 reservoirs, particularly during spring and early summer, reflecting the influence of catchment hydrology
370 and episodic inputs^{12,47}. In contrast, the Sau and Susqueda reservoirs exhibited higher DOC levels,
371 particularly during summer and autumn, consistent with enhanced in-reservoir processing under
372 stratified conditions^{48,49}. At the Pastoral intake and the DWTP inlet, DOC values reflected an integrated
373 downstream signal with reduced variability, suggesting the combined influence of upstream inputs and
374 reservoir operations.

375 Correlation analyses further revealed clear spatial connectivity patterns along the continuum (Figure
376 S6). DOC at Ter River showed weak or negative correlations with downstream locations (Sau-extracted:
377 $r = 0.38$; Sqd-extracted: $r = -0.39$; PST: $r = -0.41$; DWTP-inlet: $r = -0.30$), indicating limited direct
378 propagation of upstream riverine variability. Sau exhibited only modest correlations with downstream



379 sites (Sqd-extracted: $r = 0.15$; PST: $r = 0.14$; DWTP-inlet: $r = 0.17$). In contrast, Susqueda displayed
 380 strong correlations with Pasteral and the DWTP inlet ($r = 0.94$ and $r = 0.91$, respectively), consistent
 381 with PST-DWTP inlet coupling ($r = 0.95$) and indicating that DOC variability reaching the treatment
 382 plant is primarily controlled by the lower reservoirs.

383 Comparison with surface DOC values at Sau and Susqueda reservoirs (Figure S7) showed consistently
 384 higher concentrations and greater seasonal amplitudes in the reservoir epilimnion relative to extracted
 385 waters, particularly during stratified periods. This contrast highlights the role of selective withdrawal
 386 in modulating the quantity and character of organic matter delivered downstream⁵⁰. Similar patterns
 387 were observed for surface DOC correlations (Figure S8), although relationships were generally weaker,
 388 reinforcing the relevance of withdrawal conditions for downstream water quality.



389 **Figure 3.** Seasonal distribution of DOC concentrations along the river-reservoir-DWTP continuum for
 390 the period January 2015-December 2023. Monthly boxplots are shown for the Ter River, Sau (extracted
 391 withdrawal depth), Susqueda (extracted withdrawal depth, SQD), Pasteral intake (PST), and the DWTP
 392 inlet ($n_{\text{Ter}} = 69$, $n_{\text{Sau}} = 74$, $n_{\text{Susqueda}} = 70$, $n_{\text{Pasteral}} = 81$, $n_{\text{DWTP}} = 108$).
 393

394
 395 Together, these analyses indicate that DOC variability at the DWTP inlet is strongly linked to conditions
 396 at Susqueda. This longitudinal connectivity identifies Susqueda as the key upstream control point for
 397 organic matter dynamics affecting the treatment plant. Given the availability of high-frequency
 398 monitoring at this location, fDOM measured at the extraction depth was retained as a proxy to



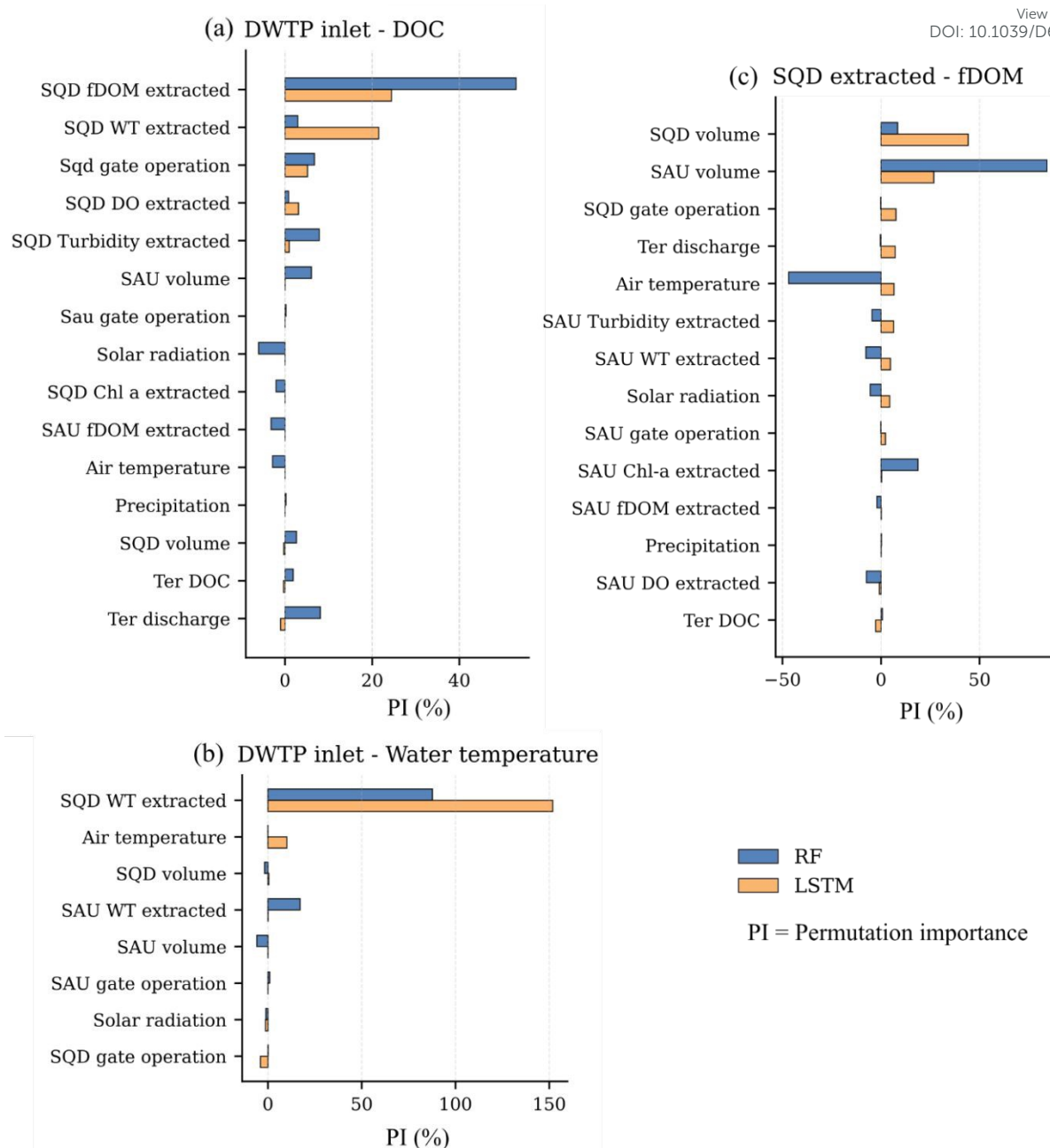
399 investigate short-term organic matter dynamics. In combination with DOC and water temperature
400 measured at the DWTP inlet, these results define the three variables selected for subsequent analysis of
401 upstream drivers, predictability and THM formation risk.

View Article Online
DOI: 10.1039/D6EW00128A

402 **3.3. Driver attribution of water quality indicators**

403 Figure 4 presents the PI results obtained using RF and LSTM models for the three selected target
404 variables: DOC, water temperature, and fDOM. Although absolute importance values differed between
405 models, both approaches revealed consistent patterns in the dominant drivers and their relative
406 influence.





407

408 **Figure 4.** Feature contributions to predict (a) DOC at the DWTP inlet, (b) Water temperature (WT) at
 409 the DWTP inlet, and (c) fDOM at Susqueda extracted withdrawal depth. Permutation importance
 410 ($\Delta R^2, \%$) was computed on the validation period for both Random Forest (RF) and Long Short-Term
 411 Memory (LSTM) models; positive values indicate important predictors, whereas negative values
 412 indicate negligible or unstable contributions.

413

414 At the DWTP inlet, DOC variability was primarily associated with water quality conditions at the
 415 Susqueda withdrawal depth, with extracted fDOM at Susqueda emerging as the most influential
 416 predictor in both RF and LSTM models (Figure 4a). Additional contributions from DO, turbidity, water
 417 temperature and gate operation at Susqueda suggested that DOC reaching the DWTP reflects organic



418 matter characteristics shaped within the reservoir and transmitted downstream through selective
419 withdrawal operations. Together, these variables represent optical properties, particulate inputs, and
420 temperature-dependent processes, which may provide complementary information beyond DOC alone,
421 as DOM responses can be linked to internal biological and physical controls that vary with stratification
422 and residence time in reservoirs^{51,52}. The higher DOC concentrations observed in the reservoirs relative
423 to the upstream Ter River (Section 3.2) further indicate a substantial autochthonous component to
424 organic matter dynamics, consistent with the elevated importance of in-reservoir water quality variables
425 in the LSTM model⁵³. In contrast, Ter River DOC and discharge showed weak or negligible
426 contributions in the LSTM but slightly higher relevance in RF, reflecting methodological differences
427 whereby RF captures static cross-sectional associations while LSTM emphasizes predictors that
428 improve temporal forecasts across lag structures⁵⁴.

429 For water temperature at the DWTP inlet (Figure 4b), PI results clearly identified water temperature at
430 the Susqueda extraction depth as the dominant driver, particularly in the LSTM model. Air temperature
431 contributed to a lesser extent, while other upstream hydrometeorological variables had minimal
432 explanatory power. This pattern indicated that thermal conditions at the DWTP were largely controlled
433 by selective withdrawal at Susqueda, with meteorological forcing indirectly embedded in the reservoir
434 thermal structure rather than acting as a direct driver at the inlet⁵⁵.

435 At Susqueda reservoir, fDOM was modeled as an independent target variable to better understand
436 controls on organic matter quality at this key upstream location (Figure 4c). PI analysis highlighted
437 reservoir storage volume as a major driver of fDOM variability, alongside withdrawal-related variables.
438 This suggests that fDOM dynamics at Susqueda are closely linked to hydrodynamic and stratification
439 conditions that regulate internal organic matter production, residence time, and vertical distribution⁵⁶.
440 The importance of storage volume was consistent with findings by Mercado-Bettín et al., 2025, who
441 reported a similar role of volume in controlling fDOM dynamics at the Sau reservoir, where water
442 volume acted as a surrogate for in-reservoir DOM production, with lower volumes associated with
443 reduced fDOM and higher volumes corresponding to increased and more stable values. The agreement



444 between studies indicates that, in large managed reservoirs, water availability and storage conditions
445 may shift DOM control from catchment-derived inputs toward internal biogeochemical processing.

446 Overall, RF and LSTM models yielded coherent driver rankings. RF provided an interpretable baseline
447 of predictor relevance in a highly correlated system, while LSTM emphasized predictors that
448 consistently improve temporal forecasts, reducing the apparent role of weaker or collinear variables.
449 Across all target variables, Susqueda reservoir operational and withdrawal-related variables emerged
450 as the dominant controls, underscoring the central role of reservoir management in shaping organic
451 matter and thermal conditions that propagate to the DWTP inlet and influence THM formation risk.

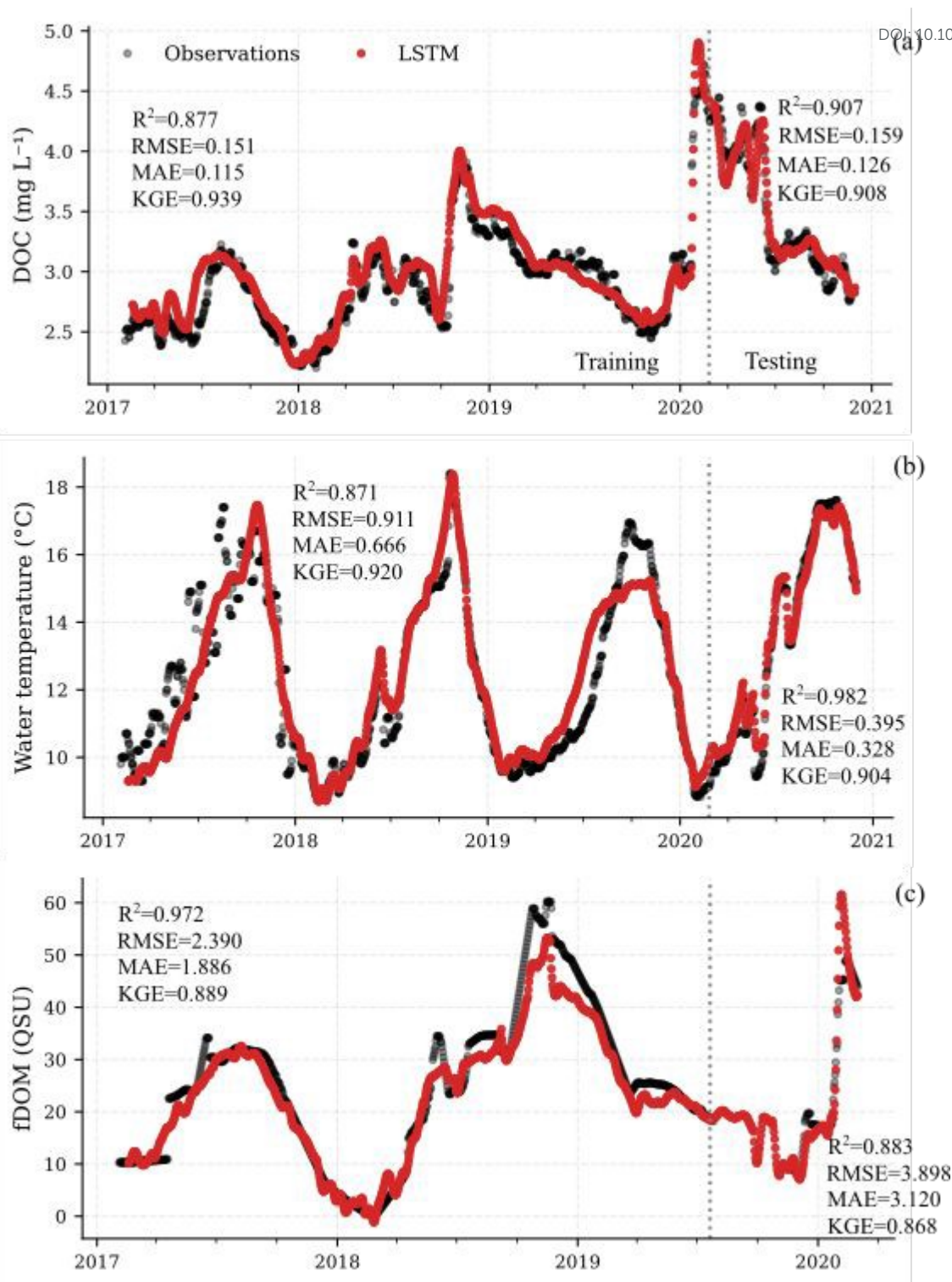
452 It should be noted that PI estimates may be affected by multicollinearity among predictors, which can
453 lead to shared or redistributed importance across correlated variables. Therefore, results are interpreted
454 in terms of consistent patterns across predictors and modeling approaches rather than as precise
455 quantitative measures of individual variable influence. This is particularly relevant in environmental
456 systems where many drivers are interdependent³⁴.

457 3.4. LSTM prediction performance

458 Time series comparisons between observations and LSTM predictions (Figure 5) illustrate the
459 predictive skill of the optimized models for DOC, water temperature, and fDOM across both training
460 and validation periods. Overall, the LSTM models closely reproduced the timing and magnitude of
461 variability, capturing both seasonal patterns and short-term fluctuations, and maintained strong
462 performance during the validation period despite increased variability and the occurrence of extreme
463 conditions.

View Article Online
DOI: 10.1039/D6EW00128A





464

465 **Figure 5.** Observed and predicted daily time series for the three modeled water quality indicators using
 466 the optimized LSTM models: (a) DOC at the DWTP inlet, (b) water temperature at the DWTP inlet,
 467 and (c) fDOM at the Susquehanna reservoir withdrawal depth. Black points show observations and the red
 468 line shows LSTM predictions. The vertical dashed line separates the training and testing periods.
 469 Performance statistics (R^2 , RMSE, MAE, KGE) are reported for each period within each panel. Note
 470 that fDOM (panel c) covers a shorter record with observational gaps due to profiler availability, whereas
 471 DOC and water temperature are continuous over February 2017–November 2020.



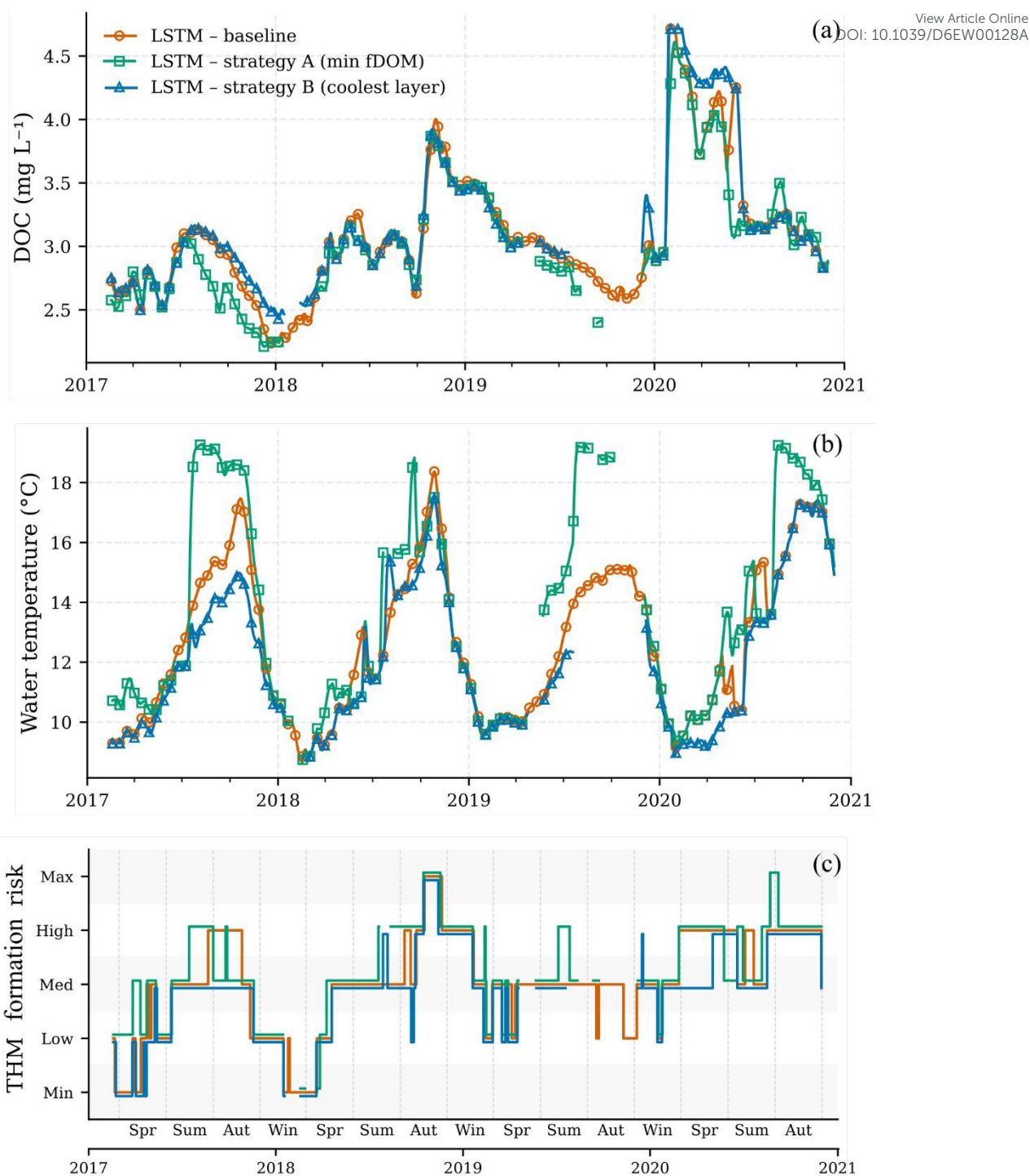
472
473 For DOC at the DWTP inlet, the highest predictability was achieved using a multivariate configuration
474 comprising ten predictors dominated by Susqueda withdrawal water quality variables (fDOM, water
475 temperature, DO, turbidity and Chl-a), together with extracted fDOM at Sau, reservoir storage volumes,
476 and upstream river inputs (DOC and discharge). Water temperature at the DWTP inlet predictions
477 required a simpler configuration, with Susqueda withdrawal temperature as the dominant predictor and
478 air temperature providing secondary information. The strong performance obtained with this minimal
479 configuration highlights the deterministic nature of downstream thermal dynamics once withdrawal-
480 layer temperature was accounted for. In contrast, fDOM predictions at the Susqueda withdrawal depth
481 required a broader predictor set to achieve optimal performance. The best results were obtained using
482 all predictors retained from the PI analysis, with the exception of precipitation, which did not improve
483 predictive skill, likely due to collinearity with river discharge and storage dynamics⁴³. This result
484 reflects the greater complexity of organic matter quality dynamics within the reservoir, which are
485 influenced by interacting processes.

486 These results demonstrated that the LSTM models effectively translated the dominant drivers identified
487 in Section 3.3 into robust generalizable predictions, while revealing clear contrasts in the number and
488 type of predictors required to optimally predict each target variable.

489 **3.5. Scenario-based simulations of reservoir operation and impacts on THM formation risk**

490 Scenario-based simulations were conducted to explore how alternative selective withdrawal strategies
491 at the Susqueda reservoir could influence DOC and water temperature at the DWTP inlet, and
492 consequently lead to shifts in THM formation risk classes (Figure 6). The baseline record reflected that
493 historical gate selection was not governed by a single formal decision rule, but rather by expert judgment
494 and system conditions. In particular, the accessible withdrawal layers were constrained by reservoir
495 water level and discrete gate availability (Figure S3), indicating that storage dynamics condition when
496 (and whether) certain operational strategies can be implemented.





497

498 **Figure 6.** Evaluation of two alternative operational withdrawal strategies using the trained LSTM
 499 models. Strategy A (organic matter-oriented) selects the Susqueda withdrawal depth associated with
 500 the minimum fDOM, whereas Strategy B (temperature-oriented) selects the coolest available layer. The
 501 strategies were propagated through the (a) DOC and (b) water temperature forecasting models to assess
 502 potential trade-offs, and the resulting DOC and water temperature simulations were combined to
 503 estimate (c) the total trihalomethane (THM) formation risk class at the DWTP inlet using the DOC-
 504 temperature risk classes proposed by Godo-Pla et al., 2021. Strategy A (green) and Strategy B (blue)
 505 are compared against the baseline scenario (red), which represents simulated historical operating
 506 conditions. Scenario trajectories include gaps for dates when the required withdrawal-depth and profiler
 507 inputs were unavailable.



508
509 Across the simulation period, the two operational strategies did not produce uniform benefits and did
510 not always concur. The “minimum fDOM” strategy (Strategy A; Figure 6a) tended to reduce predicted
511 DOC relative to baseline during selected periods, whereas the “coolest layer” strategy (Strategy B;
512 Figure 6b) more consistently reduced predicted water temperature during stratified seasons. Because
513 the THM formation risk class depends on both DOC and water temperature, a strategy only reduced
514 risk when it lowered the variable that mattered most at that time. As a result, some periods showed a
515 clear benefit from one strategy but little change from the other, while in other periods both strategies
516 produced similar outcomes, especially when baseline conditions were already close to a risk-class
517 threshold (Figure 6c).

518 The results indicate that both strategies can reduce THM formation risk relative to baseline conditions,
519 but their effectiveness varies seasonally and depends on prevailing reservoir stratification. Two
520 windows illustrate the potential for operational mitigation in this system. During summer-autumn 2017
521 and summer-autumn 2020 the simulations indicate that THM formation risk could have been reduced
522 relative to baseline (Figure 6c). These windows align with conditions where late summer stratification
523 and subsequent hydro-meteorological transitions can elevate risk; DOC can increase sharply after first
524 post-summer rainfall events, while water temperature may remain relatively high, together shifting the
525 system into higher risk categories. This pattern was consistent with seasonal behavior previously
526 reported for DOC dynamics in the Ter catchment and with the sensitivity of Mediterranean systems to
527 “first flush” events following dry periods^{45,57}. In these periods, strategy A was more effective when
528 DOC reductions were sufficient to shift the DOC class downward, while strategy B was more effective
529 when reducing temperature shifted the temperature class or prevented transitions to the highest-risk
530 combination.

531 A key insight from the scenario analysis was that optimizing DOC and temperature simultaneously was
532 not always possible because the importance of individual drivers can diverge seasonally. Although DOC
533 and water temperature at the DWTP inlet were positively associated with THM concentrations at the
534 plant and are therefore useful practical indicators of formation risk²⁵, their dominant upstream control



535 at Susquehanna may oppose each other during stratification. For example, cooler withdrawal layers can at
536 times be associated with different organic matter quality signals than surface waters, and periods that
537 minimize fDOM at the withdrawal depth may not coincide with the coolest available layer^{58,59}. This
538 helped explain why the two strategies diverged in some seasons (Figure 6a-b) and highlights the value
539 of the predictive framework for decision support. Rather than relying on a single “rule-of-thumb”,
540 managers can evaluate the trade-off between lowering DOC-related risk versus lowering temperature-
541 related risk in real time, conditional on current stratification and gate availability⁶⁰.

542 From an operational perspective, the results suggest a pragmatic approach. When the objective is short-
543 term reduction of THM formation risk categories, managers could prioritize the strategy that targets the
544 limiting component of risk at that moment. For example, strategy A during periods when DOC is near
545 a class threshold and likely to increase (e.g., post-summer rainfall transitions), and strategy B during
546 periods when temperature dominates risk (e.g., warm stratified conditions when DOC is relatively
547 stable). However, the baseline record (Figure S3), emphasizes that these decisions are sometimes
548 constrained by reservoir storage dynamics, which determine the set of withdrawal options available at
549 any given time and are influenced by system-wide release requirements⁶⁰. Therefore, the most
550 actionable implication may be that source water quality management should be coordinated with water
551 quantity governance¹. Maintaining storage conditions that preserve selective withdrawal flexibility
552 (when feasible) may increase the capacity to mitigate DBP precursor export during high-risk seasons
553^{59,61}. Under increasing drought pressure and more variable inflows, integrating reservoir operations for
554 both supply reliability and water quality may become essential to sustain risk reduction opportunities
555^{62,63}.

556 The simulated withdrawal strategies represent operationally feasible alternatives within the Ter
557 reservoir system, as they were based on observed profiler data and reflect physically accessible
558 withdrawal conditions under given reservoir water levels. Their feasibility is therefore primarily
559 determined by reservoir storage conditions, which control the availability of intake gates, while broader
560 water management objectives influence these strategies indirectly through their effect on reservoir
561 storage.



562 3.6. Study limitations and transferability

View Article Online
DOI: 10.1039/D6EW00128A

563 A key limitation of the modeling framework is the restricted temporal coverage of the dataset used for
564 model training and evaluation (2017-2020), imposed by the availability of high-frequency reservoir
565 profiler data required to represent withdrawal-depth conditions. Although this period captures a range
566 of hydroclimatic conditions, including extreme events such as Storm Gloria, it does not fully represent
567 longer-term variability, particularly the prolonged drought conditions observed after 2020. As a result,
568 model predictions and scenario simulations should be interpreted within the range of observed
569 conditions, and caution is required when extrapolating beyond this domain. Furthermore, the estimated
570 risk reductions depend on the predictive accuracy of the LSTM models and should therefore be
571 interpreted as relative, scenario-based outcomes rather than exact forecasts.

572 In addition, the use of DOC and water temperature as indicators represents a simplified description of
573 potential DBP formation processes and does not explicitly account for other influencing factors such as
574 halides, pH, or disinfectant conditions which are typically included in DBP formation models applied
575 within treatment plants and distribution systems^{64,65}. The relevance of these indicators is therefore
576 system-specific and should be assessed for each case study, particularly in systems with higher halide
577 concentrations or other relevant DBP precursors.

578 A more comprehensive assessment of uncertainty, including contributions from input data, initial
579 conditions, model parameters, and model structure, was beyond the scope of this study but represents
580 an important direction for future work.

581 Despite these limitations, the consistency between long-term exploratory analyses and model-derived
582 drivers supports the robustness of the identified control points, highlighting the value of the framework
583 for operational decision support under observed system conditions. This is particularly relevant given
584 that only a limited number of recent studies have applied ML approaches to model DOM dynamics
585 (e.g., fDOM) in reservoirs^{36,66}, which typically focus on surface conditions and meteorological forcing
586 due to data limitations and the complexity of representing internal reservoir processes.

587 4. Conclusions



588 This study demonstrates that pre-treatment DBP formation risk in a Mediterranean drinking water
589 system is strongly shaped by upstream hydroclimatic conditions, reservoir processes, and operational
590 decisions, highlighting the limitations of treatment-plant-focused approaches when applied in isolation.
591 By integrating long-term monitoring data with machine learning, the results showed that conditions in
592 key upstream reservoirs can dominate downstream variability in DBP-relevant indicators, highlighting
593 reservoirs as active control points rather than passive buffers in drinking water supply systems.

594 In the Ter system, this control was exerted by the Susqueda reservoir, where longitudinal connectivity
595 and operational choices primarily governed DOM dynamics at the drinking water treatment plant inlet.
596 Strong covariation of DOM proxies supported the use of DOC as an operationally relevant indicator,
597 while withdrawal-depth fDOM and temperature emerged as dominant drivers, emphasizing the
598 importance of vertical reservoir structure and selective abstraction. The high predictive skill achieved
599 for DOC, water temperature, and fDOM using LSTM models further indicates that data-driven
600 approaches can effectively capture the combined influence of climate variability, storage dynamics, and
601 operations in complex, managed catchment systems.

602 Scenario simulations revealed that upstream operational strategies, such as selective withdrawal, can
603 reduce indicator-based THM formation risk at the DWTP inlet, but only within specific seasonal and
604 hydroclimatic windows. The effectiveness of these interventions was constrained by reservoir levels,
605 stratification state, and infrastructure limitations, emphasizing that water quality objectives must be
606 coordinated with water quantity governance under increasing hydroclimatic stress.

607 Beyond the Ter system, this work highlights a broader and transferable opportunity for drinking water
608 utilities. While the empirical risk relationships and operational constraints are site-specific, the overall
609 framework (combining multi-source monitoring data, indicator-based risk metrics, machine learning,
610 and scenario analysis) is broadly applicable to other reservoir systems. Many treatment plants already
611 collect long-term and increasingly high-frequency data on hydrology, reservoir conditions, and raw
612 water quality, and the integration of these datasets with globally available climate data products enables
613 site-specific, data-driven analyses to support anticipatory DBP formation risk management. When
614 combined with local knowledge of infrastructure and operating constraints, such approaches offer a



615 practical pathway to move from reactive end-of-pipe mitigation toward proactive, multi-barrier
616 strategies that begin at the source. As climate change continues to intensify hydroclimatic variability,
617 leveraging existing data and integrated modeling and forecasting frameworks will be essential for
618 safeguarding drinking water quality across diverse regions.

619

620 **Author contributions**

621 Angela Pedregal-Montes: Writing-original draft, Methodology, Investigation, Formal analysis,
622 Data curation. Eleanor Jennings: Writing-review & editing, Supervision, Conceptualization,
623 Investigation, visualization. Rafael Marcé: Writing-review & editing, Conceptualization,
624 visualization, Funding acquisition. Maria José Farré: Writing-review & editing, Supervision.

625 **Conflicts of interest**

626 There are no conflicts to declare.

627 **Data availability**

628 This study used publicly available meteorological reanalysis data from the Copernicus Climate Data
629 Store (<https://cds.climate.copernicus.eu/>) and hydrological data for the catchment provided by the
630 Catalan Water Agency (ACA) through the [SDIM](#) platform. Water quality data were supplied by the
631 ATL water company and are not publicly available due to access restrictions. Data analysis and
632 machine-learning modeling were performed in Python; the specific libraries used are listed in the
633 Supplementary Information (SI). References cited in the SI are included in the article's reference list<sup>67–
634 70</sup>.

635 **Acknowledgements**

636 This project was funded by the European Union's Horizon 2020 research and innovation programme
637 under the Marie Skłodowska-Curie grant agreement no. 956623 (MSCA-ITN-ETN-European Training
638 Network, inventWater).



639 **References**

- 640 1 I. Delpla, A. V. Jung, E. Baures, M. Clement and O. Thomas, Impacts of climate change on
641 surface water quality in relation to drinking water production, *Elsevier Ltd*, 2009, preprint,
642 DOI: 10.1016/j.envint.2009.07.001.
- 643 2 B. Ma, C. Hu, J. Zhang, M. Ulbricht and S. Panglisch, Impact of Climate Change on Drinking
644 Water Safety, *ACS Environmental Science and Technology Water*, 2022, **2**, 259–261.
- 645 3 R. I. Woolway, Y. Zhang, E. Jennings, T. Zohary, S. F. Jane, J. Jansen, G. A. Weyhenmeyer,
646 D. Long, A. Fleischmann, L. Feng, B. Qin, K. Shi, H. Shi, W. Wang, Y. Tong, G. Zhang, J.
647 Zscheischler, Z. Ren and E. Jeppesen, Extreme and compound events in lakes, *Springer*
648 *Nature*, 2025, preprint, DOI: 10.1038/s43017-025-00710-w.
- 649 4 X. Liu, L. Chen, M. Yang, C. Tan and W. Chu, The occurrence, characteristics, transformation
650 and control of aromatic disinfection by-products: A review, *Elsevier Ltd*, 2020, preprint, DOI:
651 10.1016/j.watres.2020.116076.
- 652 5 I. Evlampidou, L. Font-Ribera, D. Rojas-Rueda, E. Gracia-Lavedan, N. Costet, N. Pearce, P.
653 Vineis, J. J. K. Jaakkola, F. Delloye, K. C. Makris, E. G. Stephanou, S. Kargaki, F. Kozisek, T.
654 Sigsgaard, B. Hansen, J. Schullehner, R. Nahkur, C. Galey, C. Zwiener, M. Vargha, E. Righi,
655 G. Aggazzotti, G. Kalnina, R. Grazuleviciene, K. Polanska, D. Gubkova, K. Bitenc, E. H.
656 Goslan, M. Kogevinas and C. M. Villanueva, Trihalomethanes in drinking water and bladder
657 cancer burden in the European Union, *Environ. Health Perspect.*, DOI:10.1289/EHP4495.
- 658 6 I. Kalita, A. Kamilaris, P. Havinga and I. Reva, Assessing the Health Impact of Disinfection
659 Byproducts in Drinking Water, *ACS ES and T Water*, 2024, **4**, 1564–1578.
- 660 7 S. D. Richardson, M. J. Plewa, E. D. Wagner, R. Schoeny and D. M. DeMarini, Occurrence,
661 genotoxicity, and carcinogenicity of regulated and emerging disinfection by-products in
662 drinking water: A review and roadmap for research, 2007, preprint, DOI:
663 10.1016/j.mrrev.2007.09.001.
- 664 8 S. E. Hrudey, B. Conant, I. P. Douglas, J. Fawell, T. Gillespie, D. Hill, W. Leiss, J. B. Rose
665 and M. Sinclair, Managing uncertainty in the provision of safe drinking water, *Water Sci.*
666 *Technol. Water Supply*, 2011, **11**, 675–681.
- 667 9 Y. Zhang, J. Deng, B. Qin, G. Zhu, Y. Zhang, E. Jeppesen and Y. Tong, Importance and
668 vulnerability of lakes and reservoirs supporting drinking water in China, *Fundamental*
669 *Research*, 2023, **3**, 265–273.
- 670 10 R. Xiao, Y. Deng, Z. Xu and W. Chu, Disinfection Byproducts and Their Precursors in
671 Drinking Water Sources: Origins, Influencing Factors, and Environmental Insights,
672 *Engineering*, DOI:10.1016/j.eng.2023.08.017.
- 673 11 S. Chowdhury, P. Champagne and P. J. McLellan, Models for predicting disinfection
674 byproduct (DBP) formation in drinking waters: A chronological review, 2009, preprint, DOI:
675 10.1016/j.scitotenv.2009.04.006.
- 676 12 A. Pedregal-Montes, E. Jennings, D. Kothawala, K. Jones, J. Sjöstedt, S. Langenheder, R.
677 Marcé and M. J. Farré, Disinfection by-product formation potential in response to variability in



- 678 dissolved organic matter and nutrient inputs: Insights from a mesocosm study, *Water Res.* View Article Online
 679 DOI:10.1016/j.watres.2024.121791. DOI: 10.1039/D6EW00128A
- 680 13 A. Kozari and D. Voutsas, Impact of climate change on formation of nitrogenous disinfection
 681 by products. Part I: Sea level rise and flooding events, *Science of the Total Environment*,
 682 DOI:10.1016/j.scitotenv.2023.166041.
- 683 14 A. Kozari, S. Gkellis and D. Voutsas, Impact of climate change on formation of nitrogenous
 684 disinfection by-products. Part II: water blooming and enrichment by humic substances,
 685 *Environmental Science and Pollution Research*, DOI:10.1007/s11356-024-32960-4.
- 686 15 S. Chowdhury, Adaptation of water treatment processes for controlling disinfection byproducts
 687 in supply waters to compensate the effects of climate change, *Journal of Water Process*
 688 *Engineering*, DOI:10.1016/j.jwpe.2024.105081.
- 689 16 IPCC, *Climate Change*, 2023.
- 690 17 R. Swinamer, L. E. Anderson, D. Redden, P. Bjorndahl, J. Campbell, W. H. Krkošek and G.
 691 A. Gagnon, Climate-Driven Increases in Source Water Natural Organic Matter: Implications
 692 for the Sustainability of Drinking Water Treatment, *Environ. Sci. Technol.*, 2024, **58**, 11958–
 693 11969.
- 694 18 D. Y. Dorado-Guerra, J. Paredes-Arquiola, M. Á. Pérez-Martín, G. Corzo-Pérez and L. Ríos-
 695 Rojas, Effect of climate change on the water quality of Mediterranean rivers and alternatives to
 696 improve its status, *J. Environ. Manage.*, DOI:10.1016/j.jenvman.2023.119069.
- 697 19 R. Bhattacharya, J. R. Jones, J. L. Graham, D. V. Obrecht, A. P. Thorpe, J. D. Harlan and R. L.
 698 North, Nonlinear multidecadal trends in organic matter dynamics in Midwest reservoirs are a
 699 function of variable hydroclimate, *Limnol. Oceanogr.*, 2022, **67**, 2531–2546.
- 700 20 A. Senatore, G. A. Corrente, E. L. Argento, J. Castagna, M. Micieli, G. Mendicino, A.
 701 Beneduci and G. Botter, Seasonal and Storm Event-Based Dynamics of Dissolved Organic
 702 Carbon (DOC) Concentration in a Mediterranean Headwater Catchment, *Water Resour. Res.*,
 703 DOI:10.1029/2022WR034397.
- 704 21 G. A. Weyhenmeyer and J. Karlsson, Nonlinear response of dissolved organic carbon
 705 concentrations in boreal lakes to increasing temperatures, *Limnol. Oceanogr.*, 2009, **54**, 2513–
 706 2519.
- 707 22 V. Krysanova and J. G. Arnold, Advances in ecohydrological modelling with SWAT - A
 708 review, 2008, preprint, DOI: 10.1623/hysj.53.5.939.
- 709 23 F. Alizadeh, M. H. Niksokhan, M. R. Nikoo, A. Mishra, M. Al-Wardy and G. Al-Rawas,
 710 Enhancing water security through integrated decision-making and selective withdrawal for
 711 sustainable reservoir management, *Sci. Rep.*, DOI:10.1038/s41598-025-18027-5.
- 712 24 X. C. Nguyen, V. K. H. Bui, K. H. Cho and J. Hur, Practical application of machine learning
 713 for organic matter and harmful algal blooms in freshwater systems: A review, *Taylor and*
 714 *Francis Ltd.*, 2024, preprint, DOI: 10.1080/10643389.2023.2285691.
- 715 25 L. Godo-Pla, J. J. Rodríguez, J. Suquet, P. Emiliano, F. Valero, M. Poch and H. Monclús,
 716 Control of primary disinfection in a drinking water treatment plant based on a fuzzy inference
 717 system, *Process Safety and Environmental Protection*, 2021, **145**, 63–70.



- 718 26 J. Suquet, L. Godo-Pla, M. Valentí, L. Ferrández, M. Verdaguer, M. Poch, M. J. Martín and H. Monclús, Assessing the effect of catchment characteristics to enhanced coagulation in drinking water treatment: RSM models and sensitivity analysis, *Science of the Total Environment*, DOI:10.1016/j.scitotenv.2021.149398.
- 719
- 720
- 721
- 722 27 H. Hersbach, B. Bell, P. Berrisford, S. Hirahara, A. Horányi, J. Muñoz-Sabater, J. Nicolas, C. Peubey, R. Radu, D. Schepers, A. Simmons, C. Soci, S. Abdalla, X. Abellan, G. Balsamo, P. Bechtold, G. Biavati, J. Bidlot, M. Bonavita, G. De Chiara, P. Dahlgren, D. Dee, M. Diamantakis, R. Dragani, J. Flemming, R. Forbes, M. Fuentes, A. Geer, L. Haimberger, S. Healy, R. J. Hogan, E. Hólm, M. Janisková, S. Keeley, P. Laloyaux, P. Lopez, C. Lupu, G. Radnoti, P. de Rosnay, I. Rozum, F. Vamborg, S. Villaume and J. Thépaut, The ERA5 global reanalysis, *Quarterly Journal of the Royal Meteorological Society*, 2020, **146**, 1999–2049.
- 723
- 724
- 725
- 726
- 727
- 728
- 729 28 M. N. Futter, M. A. Erlandsson, D. Butterfield, P. G. Whitehead, S. K. Oni and A. J. Wade, PERSiST: A flexible rainfall-runoff modelling toolkit for use with the INCA family of models, *Hydrol. Earth Syst. Sci.*, 2014, **18**, 855–873.
- 730
- 731
- 732 29 M. N. Futter, D. Butterfield, B. J. Cosby, P. J. Dillon, A. J. Wade and P. G. Whitehead, Modeling the mechanisms that control in-stream dissolved organic carbon dynamics in upland and forested catchments, *Water Resour. Res.*, DOI:10.1029/2006WR004960.
- 733
- 734
- 735 30 A. Pedregal-Montes, D. Mercado-Bettín, M. Futter, J. L. J. Ledesma, M. J. Farré, R. Marcé and E. Jennings, Seasonal forecasting of dissolved organic carbon in a Mediterranean catchment: Enhancing upstream control of disinfection by-product precursors, *Environ. Monit. Assess.* Submitted.
- 736
- 737
- 738
- 739 31 E. Ryder, E. Jennings, E. de Eyto, M. Dillane, C. NicAonghusa, D. C. Pierson, K. Moore, M. Rouen and R. Poole, Temperature quenching of CDOM fluorescence sensors: temporal and spatial variability in the temperature response and a recommended temperature correction equation, *Limnol. Oceanogr. Methods*, 2012, **10**, 1004–1010.
- 740
- 741
- 742
- 743 32 E. Berdalet, C. Marrasé and J. L. Pelegrí, Resumen sobre la Formación y Consecuencias de la Borrasca Gloria (19-24 enero 2020), 2020, preprint, DOI: 10.20350/digitalCSIC/12496.
- 744
- 745 33 M. Zhu, J. Wang, X. Yang, Y. Zhang, L. Zhang, H. Ren, B. Wu and L. Ye, A review of the application of machine learning in water quality evaluation, *Elsevier B.V.*, 2022, preprint, DOI: 10.1016/j.eehl.2022.06.001.
- 746
- 747
- 748 34 L. Breiman, in *Random Forest. Machine Learning*, 2001, vol. 45, pp. 5–32.
- 749 35 T. D. Harris and J. L. Graham, Predicting cyanobacterial abundance, microcystin, and geosmin in a eutrophic drinking-water reservoir using a 14-year dataset, *Lake Reserv. Manag.*, 2017, **33**, 32–48.
- 750
- 751
- 752 36 D. Mercado-Bettín, R. Paíz, V. McCarthy, E. Jennings, E. de Eyto, A. M. Gallegos, M. Dillane, J. C. Garcia, J. J. Rodríguez and R. Marcé, A machine learning approach to driver attribution of dissolved organic matter dynamics in two contrasting freshwater systems, 2025, preprint, DOI: 10.5194/egusphere-2025-4049.
- 753
- 754
- 755
- 756 37 C. Fournier, R. Fernandez-Fernandez, S. Cirés, J. A. López-Orozco, E. Besada-Portas and A. Quesada, LSTM networks provide efficient cyanobacterial blooms forecasting even with incomplete spatio-temporal data, *Water Res.*, 2024, **267**, 122553.
- 757
- 758



- 759 38 J. C. Pyo, Y. Pachepsky, S. Kim, A. Abbas, M. Kim, Y. S. Kwon, M. Ligaray and K. H. Cho, Long short-term memory models of water quality in inland water environments, *Elsevier Ltd*,
760 2023, preprint, DOI: 10.1016/j.wroa.2023.100207. View Article Online
DOI: 10.1039/D6EW00128A
- 762 39 S. Hochreiter and J. Schmidhuber, Long Short-Term Memory, *Neural Comput.*, 1997, **9**,
763 1735–1780.
- 764 40 D. Wang, C. Zhang, A. Li, Y. Guo, H. Zhang and C. Tan, Spatio-temporal analysis and
765 prediction for raw water quality of drinking water source by improved RNN algorithm,
766 *Journal of Water Process Engineering*, 2025, **71**, 107164.
- 767 41 J. Ruan, Y. Cui, Y. Song and Y. Mao, A novel RF-CEEMD-LSTM model for predicting water
768 pollution, *Sci. Rep.*, 2023, **13**, 20901.
- 769 42 C. Strobl, A. L. Boulesteix, A. Zeileis and T. Hothorn, Bias in random forest variable
770 importance measures: Illustrations, sources and a solution, *BMC Bioinformatics*,
771 DOI:10.1186/1471-2105-8-25.
- 772 43 A. Fisher, C. Rudin and F. Dominici, *All Models are Wrong, but Many are Useful: Learning a
773 Variable's Importance by Studying an Entire Class of Prediction Models Simultaneously*,
774 2019, vol. 20.
- 775 44 I. Caballero, M. Roca, M. B. Dunbar and G. Navarro, Water Quality and Flooding Impact of
776 the Record-Breaking Storm Gloria in the Ebro Delta (Western Mediterranean), *Remote Sens.
777 (Basel)*, 2023, **16**, 41.
- 778 45 J. L. J. Ledesma, A. Lupon, E. Martí and S. Bernal, Hydrology and riparian forests drive
779 carbon and nitrogen supply and DOC:g NO₃-stoichiometry along a headwater Mediterranean
780 stream, *Hydrol. Earth Syst. Sci.*, 2022, **26**, 4209–4232.
- 781 46 S. D. Richardson, Disinfection by-products and other emerging contaminants in drinking
782 water, *TrAC - Trends in Analytical Chemistry*, 2003, **22**, 666–684.
- 783 47 P. A. Raymond and R. G. M. Spencer, in *Biogeochemistry of Marine Dissolved Organic
784 Matter*, Elsevier, 2015, pp. 509–533.
- 785 48 W. Zheng, Y. Chen, Y. Niu, P. Xu, H. Hao and B. Dong, Disinfection by-product formation
786 potential in response to seasonal variations in lake water sources: Dependency on fluorescent
787 and molecular weight characteristics, *Science of the Total Environment*,
788 DOI:10.1016/j.scitotenv.2024.177891.
- 789 49 E. Munthali, R. Marcé and M. J. Farré, Drivers of variability in disinfection by-product
790 formation potential in a chain of thermally stratified drinking water reservoirs, *Environ. Sci.
791 (Camb)*, 2022, **8**, 968–980.
- 792 50 L. Cáceres, D. Méndez, J. Fernández and R. Marcé, From End-of-Pipe to Nature Based
793 Solutions: a Simple Statistical Tool for Maximizing the Ecosystem Services Provided by
794 Reservoirs for Drinking Water Treatment, *Water Resources Management*, 2018, **32**, 1307–
795 1323.
- 796 51 M. Abbasi, M. Peacock, S. Drakare, J. Hawkes, E. Jakobsson and D. Kothawala, Water
797 residence time is an important predictor of dissolved organic matter composition and drinking
798 water treatability, *Water Res.*, DOI:10.1016/j.watres.2024.121910.



- 799 52 D. W. Howard, A. G. Hounshell, M. E. Lofton, W. M. Woelmer, P. C. Hanson and C. C. Carey, Variability in fluorescent dissolved organic matter concentrations across diel to
800 seasonal time scales is driven by water temperature and meteorology in a eutrophic reservoir,
801 *Aquat. Sci.*, 2021, **83**, 30. View Article Online
DOI: 10.1039/D6EW00128A
- 803 53 Y. Wu, H. Fang, L. Huang, C. He, Q. Shi, Y. Yi, D. He and K. Wang, Reservoir operation
804 regulates the dynamics of dissolved organic matter in sediments, *J. Environ. Manage.*, 2025,
805 **392**, 126850.
- 806 54 S. Hochreiter and J. Schmidhuber, Long Short-Term Memory, *Neural Comput.*, 1997, **9**,
807 1735–1780.
- 808 55 G. Hu, Z. Yang, Y. Yue, F. Bai and Y. Ren, Joint thermal regulation by selective withdrawal
809 in serial cascade reservoir systems effectively improves reservoir and downstream ecological
810 health, *Water Res.*, 2025, **281**, 123659.
- 811 56 X. Wang, H. Zhang, E. Bertone, R. A. Stewart and S. P. Hughes, Hybrid three-dimensional
812 modelling for reservoir fluorescent dissolved organic matter risk assessment, *Inland Waters*,
813 2022, **12**, 463–476.
- 814 57 S. Bernal, A. Butturini and F. Sabater, Variability of DOC and nitrate responses to storms in a
815 small Mediterranean forested catchment, *Hydrol. Earth Syst. Sci.*, 2002, **6**, 1031–1041.
- 816 58 G. Hu, Z. Yang, Y. Yue, F. Bai and Y. Ren, Joint thermal regulation by selective withdrawal
817 in serial cascade reservoir systems effectively improves reservoir and downstream ecological
818 health, *Water Res.*, 2025, **281**, 123659.
- 819 59 B. Zouabi-Aloui, S. M. Adelana and M. Gueddari, Effects of selective withdrawal on
820 hydrodynamics and water quality of a thermally stratified reservoir in the southern side of the
821 Mediterranean Sea: a simulation approach, *Environ. Monit. Assess.*, 2015, **187**, 292.
- 822 60 E. Soyer, H. Bayram, N. Canıgeniş and O. Eren, Decision support system for selective
823 withdrawal in water supply reservoirs: an approach based on thermal stratification, *Water*
824 *Quality Research Journal*, 2023, **58**, 99–110.
- 825 61 C. A. Murphy, S. L. Johnson, W. Gerth, T. Pierce and G. Taylor, Unintended Consequences of
826 Selective Water Withdrawals From Reservoirs Alter Downstream Macroinvertebrate
827 Communities, *Water Resour. Res.*, DOI:10.1029/2020WR029169.
- 828 62 M. Nazari and R. Kerachian, Optimal Operation of Reservoirs Considering Water Quantity
829 and Quality Aspects: A Systematic State-of-the-Art Review, *Water Resources Management*,
830 2024, **38**, 5911–5944.
- 831 63 M. Reza Nikoo, N. Bahrami, K. Madani, G. Al-Rawas, S. Vanda and R. Nazari, A robust
832 decision-making framework to improve reservoir water quality using optimized selective
833 withdrawal strategies, *J. Hydrol. (Amst.)*, 2024, **635**, 131153.
- 834 64 L. Liang and P. C. Singer, Factors Influencing the Formation and Relative Distribution of
835 Haloacetic Acids and Trihalomethanes in Drinking Water, *Environ. Sci. Technol.*, 2003, **37**,
836 2920–2928.



- 837 65 S. Chowdhury, P. Champagne and P. J. McLellan, Models for predicting disinfection
838 byproduct (DBP) formation in drinking waters: A chronological review, 2009, preprint, DOI:
839 10.1016/j.scitotenv.2009.04.006. View Article Online
DOI: 10.1039/D6EW00128A
- 840 66 D. W. Howard, M. E. Lofton, R. Q. Thomas, A. D. Delany, A. Breef-Pilz and C. C. Carey,
841 Near-Term Forecasts of Dissolved Organic Matter Exhibit Consistent Patterns of Accuracy
842 Across Multiple Freshwater Reservoirs, *J. Geophys. Res. Biogeosci.*,
843 DOI:10.1029/2025JG009064.
- 844 67 M. Kuhn and K. Johnson, *Applied Predictive Modeling*, Springer New York, New York, NY,
845 2013.
- 846 68 APHA, *AWWA and WPCF Standard Methods for the Examination of Waters and Waste*
847 *Waters*, 2005.
- 848 69 T. Niedzielski and M. Halicki, Improving Linear Interpolation of Missing Hydrological Data
849 by Applying Integrated Autoregressive Models, *Water Resources Management*, 2023, **37**,
850 5707–5724.
- 851 70 Z. Che, S. Purushotham, K. Cho, D. Sontag and Y. Liu, Recurrent Neural Networks for
852 Multivariate Time Series with Missing Values, *Sci. Rep.*, 2018, **8**, 6085.
853



Data availability

This study used publicly available meteorological reanalysis data from the Copernicus Climate Data Store (<https://cds.climate.copernicus.eu/>) and hydrological data for the catchment provided by the Catalan Water Agency (ACA) through the [SDIM](#) platform. Water quality data were supplied by the ATL water company and are not publicly available due to access restrictions. Data analysis and machine-learning modeling were performed in Python; the specific libraries used are listed in the Supplementary Information (SI). References cited in the SI are included in the article's reference list^{60–63}.

